Wave-Breaking Model for Boussinesq-Type Equations Including Roller Effects in the Mass Conservation Equation

Rodrigo Cienfuegos[1]; Eric Barthélemy[2]; and Philippe Bonneton[3]

Abstract: We investigate the ability of a 1D fully nonlinear Boussinesq model including breaking to reproduce surf zone waves in terms of wave height and nonlinear intraphase properties such as asymmetry and skewness. An alternative approach for wave-breaking parameterization including roller effects through diffusive-type terms on both, the mass conservation and momentum equations is developed and validated on regular wave and solitary wave experiments as an attempt to improve wave height and left-right asymmetry estimates. The new approach is able to reproduce wave height decay, and intraphase nonlinear properties within the entire surf zone of spilling breakers without requiring temporal evolution of model parameters.

Introduction

Over the past 15 years, important practical improvements for Boussinesq-type equations have been produced extending their range of applications further into deep waters and into the surf zone. Even though the question of incorporating wave-breaking effects into such potential-like models was addressed very early, it was not until the 1990s that several attempts to parameterize this phenomenon were performed with relative success (Schäffer et al. 1993; Zelt 1991). Generally speaking, the different wave breaking approaches consider the inclusion of an extra term in the momentum equation in order to dissipate energy when wave breaking is likely to occur. Those additional ad hoc terms can be thought as a force acting on the front face of the breaker. Their practical implementation requires at least: (1) an explicit breaking criterion to activate extra terms; (2) some energetic considerations in order to relate model parameters to the energy dissipated in surf zone waves. In addition, they must ensure mass and momentum conservation and preserve nonlinear wave properties such as asymmetry and skewness.

One of the earliest attempts to incorporate breaking effects was independently proposed by Zelt (1991) and Karambas and Koutitas (1992) using an eddy viscosity analogy to write an extra term in the momentum equation. Model performance for periodic waves was only investigated by Karambas and Koutitas (1992), since Zelt (1991) applied his breaking parameterization to solitary waves. However, the Karambas and Koutitas (1992) formulation was not momentum preserving and setup prediction in the inner surf zone was very poor whereas wave height decay was reasonably computed. The latter illustrates the importance of ensuring that breaking terms only introduce a momentum deficit locally without affecting its overall surf zone budget. Only recently, Kennedy et al. (2000) were able, using the eddy viscosity analogy developed by Zelt (1991), to adequately reproduce wave height decay and setup for regular waves breaking on planar beaches.

In parallel, a different approach was followed by Brocchini et al. (1992) and Schäffer et al. (1993). Their breaking wave models were explicitly written using the Svendsen (1984) roller concept where extra terms could be linked to local roller thickness and the mean front slope of the breaker. Even though, this approach stems on very different hypothesis and ideas, the overall effect in momentum equation is equivalent to breaking models based on the eddy viscosity analogy, namely a local momentum deficit at the front of the breaker. The roller approach was further developed by Madsen et al. (1997a) and even applied to irregular wave propagation problems [e.g., Bayram and Larson (2000), Madsen et al. (1997b), and Ozanne et al. (2000)]. In addition, the roller concept also provided some theoretical background for the development of Boussinesq models with vorticity proposed recently [e.g., Briganti et al. (2004), Musumeci et al. (2005), and Veeramony and Svendsen (2000)]. Although it is not stated explicitly, those models include, through additional vortical terms, some breaking effects in the mass conservation equation.

Even though roller-based breaking models are attractive because they rely on better physical backgrounds, their numerical implementation is rather complicated and at least five different parameters must be tuned. On the other hand, using the eddy viscosity analogy results in a somewhat simpler model but no direct physical meaning can be attributed to the associated scaling coefficients. The lack of physical knowledge of breaking processes makes the task of parameterizing breaking effects very difficult since no *universal* scaling laws for physical variables

[1]Assistant Professor, Departamento de Ingeniería Hidráulica y Ambiental, Pontificia Universidad Católica de Chile, Vicuña Mackenna 4860, casilla 306, correo 221, Santiago de Chile, Chile. E-mail: racienfu@ing.puc.cl

[2]Professor, Institut National Polytechnique de Grenoble, UMR 5519 LEGI (CNRS, INPG, UJF), BP53 38041 Grenoble Cedex 9, France. E-mail: eric.barthelemy@hmg.inpg.fr

[3]Research Director, Univ. Bordeaux 1, CNRS, UMR 5805 EPOC, Av. des Facultés, Talence F-33405, France. E-mail: p.bonneton@epoc.u-bordeaux1.fr
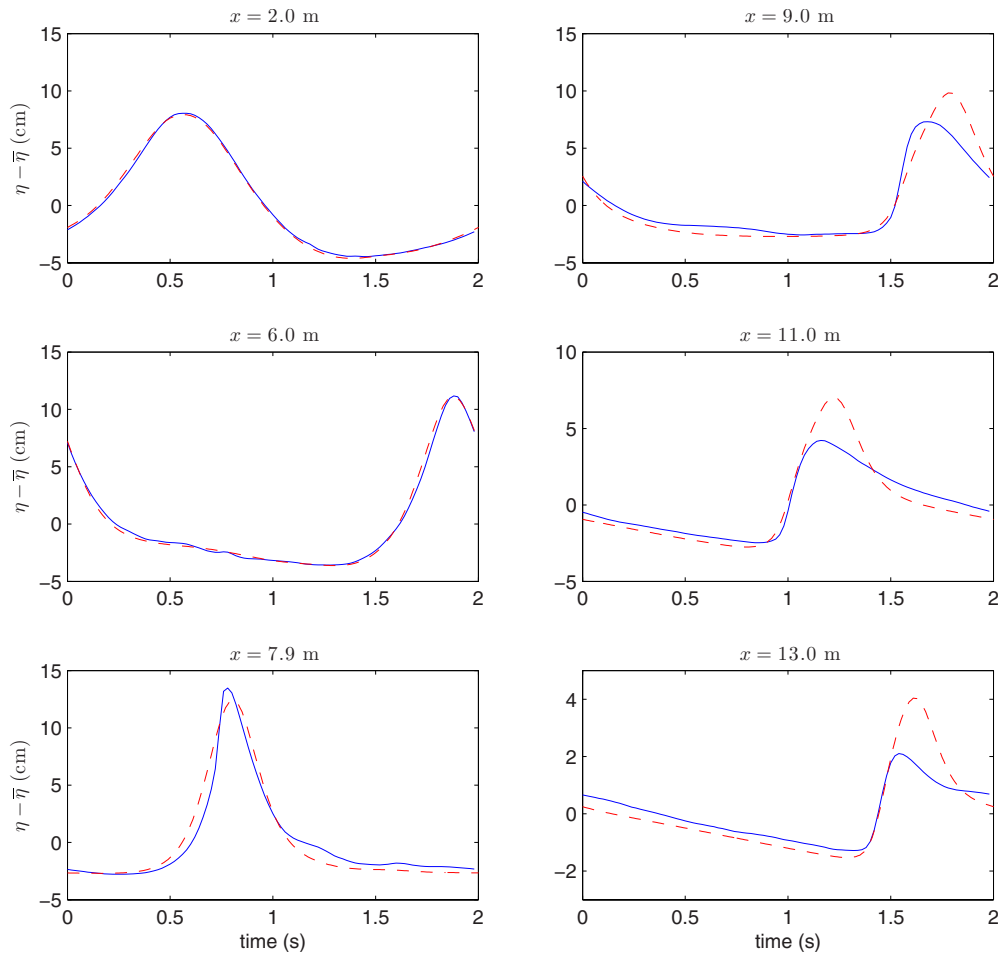
Fig. 1. Computed and measured phase-averaged time series of free-surface elevation for Ting and Kirby (1994) spilling breaking experiment at several wave gauges using Kennedy et al. (2000) parameterization with $\delta_b = 1.2$. (–): measured; (– –) computed

have been found. In this context, none of the aforementioned breaking approaches have shown a clear superiority over the others. In the present work, we aim at extending the eddy viscosity analogy, which appears to be simpler than roller-based approaches, and to correct some practical limitations observed in formerly proposed models. In addition, an attempt to relate embedded parameters to macroscopic properties of surf zone waves is also described.

In order to illustrate potential drawbacks that may limit the applicability of eddy viscosity parameterizations in time-domain modeling, we have implemented Kennedy et al. (2000) wave-breaking model in the fully nonlinear finite volume Boussinesq-type solver SERR-1D (Cienfuegos et al. 2006a,2007). In Fig. 1 we show results for the spilling breaking case reported by Ting and Kirby (1994), using default parameter values for the breaking model. An excellent agreement between computed and measured time series in the shoaling region ($x < 7.9$) is observed but important discrepancies arise inside the surf zone ($x > 7.9$) where the breaking model is active. In particular wave heights in the inner surf zone are overestimated, a drawback that was already reported by Kennedy et al. (2000). Nevertheless, left-right wave asymmetry is reasonably reproduced and wave's front slope is preserved. A detailed comparison between important measured and computed wave-averaged properties is presented in Fig. 2. In this example, the RMS errors in wave height, asymmetry, and skewness are, respectively, 17%, 40%, and 38%. The average numeri-

cal error can be estimated as the arithmetic mean of the these three quantities, giving 32% in this case.

Better wave height estimates can be obtained by increasing the amount of energy dissipation in the breaking model. This is easily achieved by increasing the mixing length parameter, δ_b [Kennedy et al. (2000), for details]. Computed results for the same spilling breaking case, but with a five times higher δ_b value, are shown in Fig. 3. Similarly, Fig. 4 presents comparisons between computed and measured wave-averaged properties where the associated RMS errors for wave height, wave asymmetry, and skewness has been estimated to be, respectively, 9%, 64%, and 17% with an average error of nearly 30%, hence not very different from the one obtained using default parameter values. Hence, even though the overall agreement between computed and measured wave height is improved, forcing the breaking model with this high δ_b value results in a significant loss of wave left-right asymmetry. This result suggests that the equivalent force that one needs to apply on the front face of the breaker in order to introduce the correct energy dissipation rate might be unrealistically strong or applied over a too large portion of the wave. Hence, Kennedy et al. (2000) eddy viscosity formulation may have some difficulties in simultaneously providing reliable predictions of wave heights and horizontal asymmetries in the inner surf zone. This important practical limitation constitutes the main motivation for developing the alternative approach described in this article.

The new wave-breaking model stems from simple energetic
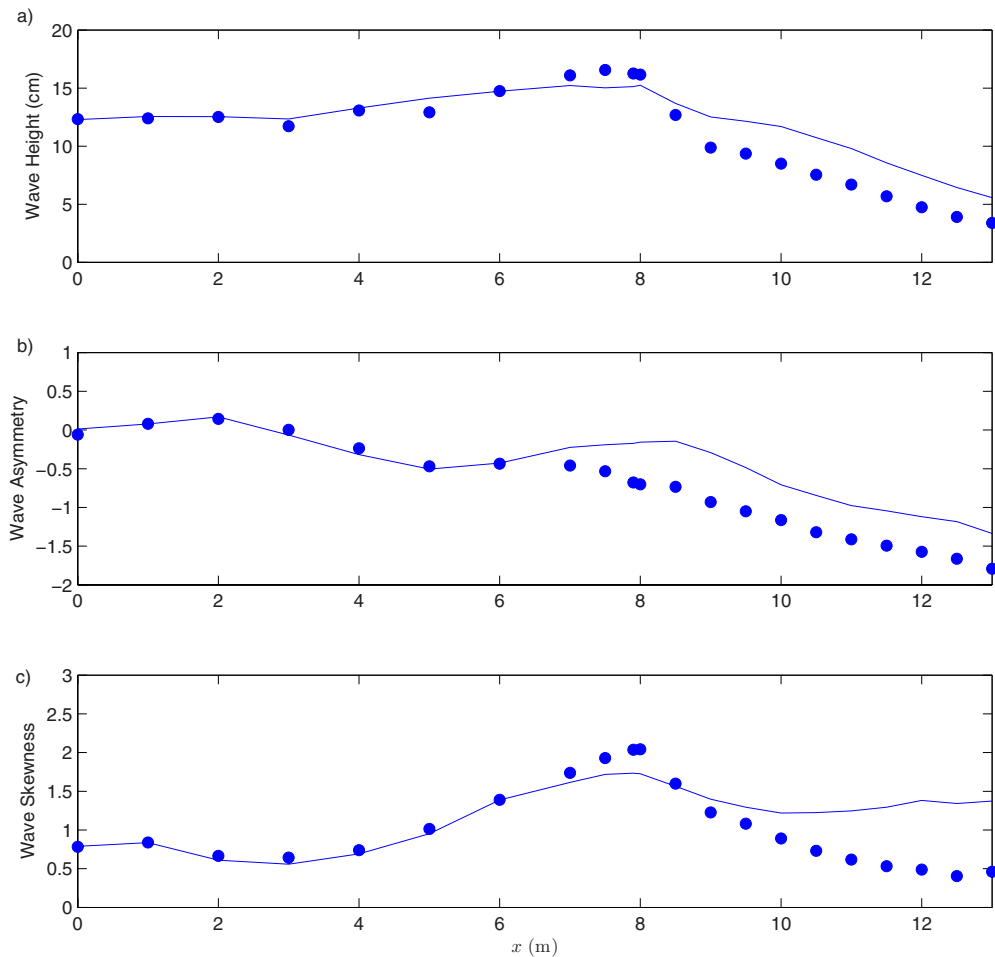
Fig. 2. Comparison between measured (●) and computed (–) wave properties for Ting and Kirby's (Ting and Kirby 1994) spilling breaking experiment using Kennedy et al. (2000) parameterization with $\delta_b = 1.2$. (a) Wave height; (b) wave asymmetry; and (c) wave skewness.
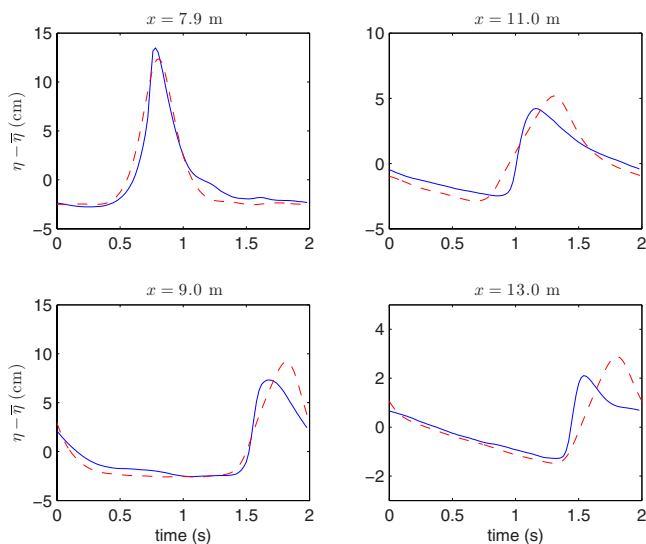
Fig. 3. Computed and measured phase-averaged time series of free-surface elevation for Ting and Kirby (1994) spilling breaking experiment at several wave gauges using Kennedy et al. (2000) parameterization with $\delta_b = 5.5$. (–): measured; (—) computed

principles and can be viewed as an extension of the eddy viscosity analogy used by Zelt (1991) and Kennedy et al. (2000). The main difference with formerly proposed models is related to the inclusion of an extra diffusivity term in the mass conservation equation.

In the first section, we review some important properties of wave-breaking parameterizations in the framework of Boussinesq-type modeling. The following section is devoted to the development, calibration, and validation of the proposed breaking model.

Problem Setting for Breaking and Dissipation in Boussinesq Models

Boussinesq-type equations constitute an essentially inviscid set, hence breaking-induced effects must be introduced in an external or ad hoc manner. In addition, a breaking criterion must be adopted to activate extra terms, and wave crests need to be followed since a wave-by-wave approach must be considered. Finally, model parameters must be scaled to ensure that the overall externally induced energy dissipation is in agreement with the rate of energy dissipated in surf zone waves.

Energetic Considerations

The Boussinesq set of equations that we will use to describe wave motion is an extension of the so-called Serre equations to uneven
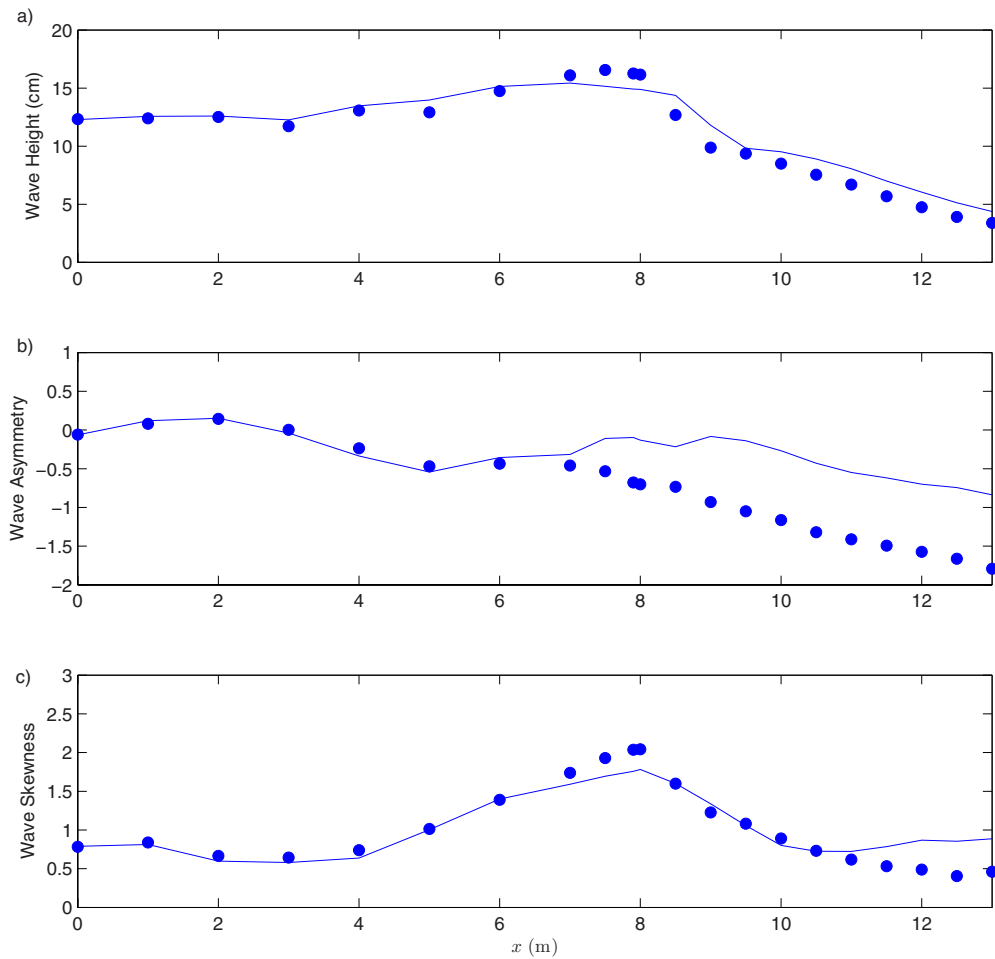
Fig. 4. Comparison between measured (●) and computed (–) wave properties for Ting and Kirby's (Ting and Kirby 1994) spilling breaking experiment using Kennedy et al.'s (Kennedy et al. 2000) parameterization with $\delta_b = 5.5$. (a) Wave height; (b) wave asymmetry; and (c) wave skewness.

bathymetries (Seabra-Santos et al. 1987) incorporating in addition a Padé (2,2) dispersion correction (Barthélemy 2004). This set of equations is actually fully nonlinear in the sense that it includes all terms up to $O(\sigma^2)$ by considering that $O(\epsilon) \sim 1$ (where $\sigma = kh_0$ and $\epsilon = a/h_0$ are respectively the dispersive and nonlinear parameters, a is the wave amplitude, h_0 is the water depth, and k is the wave number).

For horizontal bottoms and incorporating wave-breaking terms, the Boussinesq set of equations is recast in the following generic form:

$$\frac{\partial h}{\partial t} + \frac{\partial}{\partial x}(hu) - D_h = 0 \qquad (1)$$

$$\frac{\partial u}{\partial t} + \frac{1}{2}\frac{\partial u^2}{\partial x} + g\frac{\partial h}{\partial x} + \Gamma_d - \frac{1}{h}D_{hu} = 0 \qquad (2)$$

where h and u are, respectively, the local depth of the *organized* or potential bulk flow and the horizontal fluid velocity averaged over this depth (see Fig. 5), D_h and D_{hu} represent breaking-induced contributions; Γ_d contains dispersive Boussinesq-type terms [see Cienfuegos et al. (2006a), for a detailed description]; and g is the gravitational acceleration. Here variables x and t denote absolute space and time coordinates. It is important to emphasize that in the present definition a clear distinction is made between the organized layer where potential flow theory might be
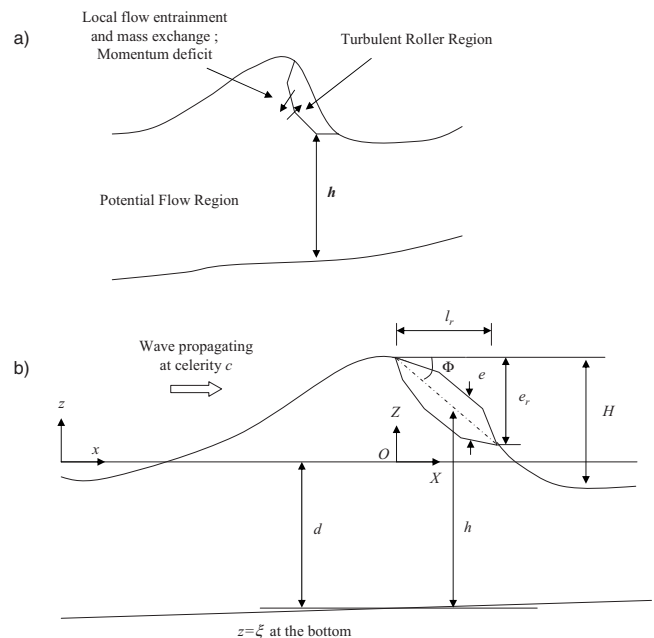
Fig. 5. Definition sketch for a breaking wave. (a) Potential and turbulent flow regions; (b) definition of related variables.

applied and the turbulent roller region that develops above it when breaking takes place.

It is worth pointing out that when the eddy viscosity analogy (Kennedy et al. 2000; Zelt 1991) is used, only the breaking-induced momentum term, D_{hu} is included. Our extra term appears because the mass conservation equation is not integrated all the way to the free surface, but only over the organized bulk flow layer. Therefore, the turbulent roller region is excluded from the definition for depth-averaged equations, so that extra breaking terms represent respectively, for the continuity and momentum equations: (1) a local mass exchange between the turbulent and potential flow regions; (2) a local momentum deficit produced by the presence of the roller (see Fig. 5).

Multiplying Eq. (1) by $gh + 1/2u^2$, Eq. (2) by hu, summing up and neglecting dispersive effects leads to the energy equation

$$\frac{\partial}{\partial t}\left[\frac{1}{2}h(gh + u^2)\right] + \frac{\partial}{\partial x}\left[hu\left(gh + \frac{1}{2}u^2\right)\right] = -\frac{\Delta_b}{\rho} \quad (3)$$

where $-\Delta_b = \rho[gh + 1/2u^2]D_h + \rho u D_{hu}$ ($\Delta_b \geq 0$), is defined as the local rate of energy dissipation (per unit width) by breaking, and ρ is the water density. In the framework of potential flow theory, it can be shown that if breaking terms are zero, energy is conserved even when dispersive effects are taken into account. A similar analysis was given by Kirby and Kaihatu (1996) on a linearized set of equations.

Using a mild slope hypothesis, the overall wave-averaged energy dissipated from the mean flow by breaking, can be reasonably computed from the nonlinear shallow water shock theory. In the moving frame of reference (O, X, Z) of the propagating bore (see Fig. 5), the total dissipated energy can thus be evaluated as (Bonneton 2001; Svendsen et al. 1978)

$$\int_{\text{shock}} \frac{\Delta_b}{\rho}dX \simeq \frac{1}{4}gc\gamma^3 d^2 \quad (4)$$

where d=mean water depth, $\gamma = H/d$ is the breaker index (with H being the wave height) and $c = \sqrt{gd}$=local celerity of the breaking wave.

Breaking Criterion

Among the different breaking criteria that have been employed in Boussinesq-type models we should cite the critical front slope introduced by Schäffer et al. (1993), a velocity gradient limit proposed by Zelt (1991) and applied to solitary waves, or a similar approach used by Kennedy et al. (2000) where the critical spatial velocity gradient is written instead in terms of the time derivative of the free surface using the continuity equation. Alternatively, a breaking criterion based on a relative trough Froude number (RTFN) was proposed by Okamoto and Basco (2006).

It has also been recognized that an additional criterion is necessary in order to decide when the breaking process stops. Breaker slope, time derivative free surface, and RTFN criterions include and explicit treatment for this situation. A heuristic law for the evolution of the mean breaker angle, Φ, in the surf zone (see Fig. 5) has been proposed by Schäffer et al. (1993)

$$\Phi = \Phi_t + (\Phi_i - \Phi_t)\exp\left[-\frac{(t - t_b)}{T_b}\log(2)\right], \quad \text{for} \quad t \geq t_b \quad (5)$$

where Φ_i and Φ_t correspond respectively to breaker angles at incipient breaking and in quasi-equilibrium (borelike) state; t_b is the time at which the wave started to break; and T_b is a characteristic transitional time scale. Schäffer et al. (1993) used Φ_t

=20°, $\Phi_t = 8$°, and $T_b = T/10$ on their weakly nonlinear Boussinesq model.

On the other hand, breaking criterion included in Kennedy et al. (2000) consists in fixing a threshold value for the free-surface time derivative, $\partial \eta^*/\partial t$, written as

$$\frac{\partial \eta^*}{\partial t} = \begin{cases} \eta_t^{(F)}, & \text{if } t - t_b \geq T_b^*, \\ \eta_t^{(I)} + \frac{(t - t_b)}{T_b^*}(\eta_t^{(F)} - \eta_t^{(I)}), & \text{if } 0 \leq t - t_b < T_b^* \end{cases} \quad (6)$$

where $\eta_t^{(I)}$ and $\eta_t^{(F)}$ correspond, respectively, to the threshold values at the breaking point and to a saturated value for breaking cessation. This criterion also considers a transitional time scale T_b^* in the surf zone. Those authors used on their fully nonlinear Boussinesq model $\eta_t^{(I)} = 0.65\sqrt{g|\xi|}$ (where $|\xi|$ is the local still water depth), $\eta_t^{(F)} = 0.15\sqrt{g|\xi|}$ and $T_b^* = 5\sqrt{|\xi|/g}$.

It is important to point out that both breaking criteria presented earlier are rather similar in essence. Indeed, using a progressive wave of constant form hypothesis, we may write

$$\frac{\partial \eta}{\partial t} + c\frac{\partial \eta}{\partial x} = 0 \quad (7)$$

which shows that the free-surface time derivative can be related, at first order, to the mean front slope of the breaker since $\partial \eta/\partial x \simeq -\tan\Phi$. It follows that threshold values for breaking initiation and cessation proposed by Kennedy et al. (2000) are roughly equivalent to mean breaker angles $\Phi_i = 33$° and $\Phi_t = 8.5$°.

It is worth noting that the threshold value for breaking initiation will be strongly dependent on the particular set of Boussinesq-type equations used to describe wave motion. This explains why the incipient breaker angle had to be fixed at $\Phi_i = 20$° by Schäffer et al. (1993), which is a much lower value than the one used in Kennedy et al. (2000) fully nonlinear model. In addition, both approaches consider the history of each breaking event by fixing a time evolving function for threshold values of Φ and $\partial \eta^*/\partial t$. This temporal dependence implies that each breaking event must be marked and followed as breakers propagate toward the shore.

New Approach for Time-Domain Breaking

In the present section we develop a new wave-breaking model for Boussinesq-type equations embracing the shallow water shock theory and the roller concept as theoretical backgrounds.

Functional Form of Breaking Terms and Scaling Arguments

Some scaling information for wave-breaking terms can be obtained if we use the long wave approximation and the assumption of a gently sloping beach. These simplifications will allow us to use some important results valid for quasi-steady breakers or bores.

Invoking shallow water shock theory a useful relation exists for the overall energy dissipated across the shock in surf zone waves. This expression was written in Eq. (4). Whereas in shock theory, the dissipation is concentrated on the discontinuity (i.e., over an infinitesimal horizontal distance), for real surf zone waves dissipation takes place over a finite distance, l_r. Hence, numerical solutions obtained using shock capturing numerical solvers have an important dependence on the spatial grid resolution, Δx, because the discrete length of the discontinuity is governed by that

parameter. Consequently, in the limit $\Delta x \to 0$, l_r must tend to zero as well. Nevertheless, real breakers never show vertical fronts so Δx must be tuned in order to correctly reproduce wave asymmetry.

Even though some important and useful results concerning the application of shock capturing methods to breaking waves in the inner surf zone have been reported [e.g., Bonneton (2007), Kobayashi et al. (1989), and Vincent et al. (2001)], successful application of these methods implicitly requires some information on the finite length l_r. Owing to this dependence on the grid resolution, we prefer to follow a different approach which incorporates an explicit estimation for this horizontal scale.

Combining the energy Eq. (3) with the theoretical result given by expression (4) we obtain, in the moving frame of reference, the following integral scaling relation for breaking terms:

$$-\int_0^{l_r}\left[\left(gh+\frac{1}{2}(U+c)^2\right)D_h+(U+c)D_{hu}\right]dX \sim \frac{1}{4}gc\gamma^3 d^2 \quad (8)$$

where l_r represents now the horizontal distance over which extra terms are nonzero and $U=u-c$ is the depth-averaged velocity in the moving frame of reference. In the rest of this section we will assume that breaking terms are of diffusive type following the model proposed by Zelt (1991). However, we incorporate an extra term in the continuity equation. As previously discussed, this extra contribution aims at introducing roller effects not taken into account by potential flow theory.

Breaking terms are thus written in the frame of reference of the propagating wave as

$$D_h = \frac{d}{dX}\left(\nu_h \frac{dh}{dX}\right) \quad (9)$$

$$D_{hu} = \frac{d}{dX}\left\{\nu_{hu}\frac{d}{dX}[h(U+c)]\right\} \quad (10)$$

where ν_h and ν_{hu} = diffusivity functions that need to be defined. Therefore, in order to integrate the left hand side of Eq. (8) some additional information must be provided. We specifically need an estimate for l_r and the local functional forms for ν_h and ν_{hu}.

Since energy dissipation can be related to shearing stresses acting on the lower edge of the roller (Dally and Brown 1995; Deigaard and Fredsøe 1989), we take l_r to be the roller length. On the other hand, experimental results on hydraulic jumps with Froude numbers close to those encountered in the inner surf zone reported by Svendsen et al. (2000) suggest that the spatial distribution for the local roller thickness and the maximum shear stress distribution are similar. We will assume then that mass and momentum diffusivity coefficients follow the same kind of relation which can be written as (Veeramony and Svendsen 2000)

$$\nu_h(X) = -K_h \exp\left(\frac{X}{l_r}-1\right)\left[\left(\frac{X}{l_r}-1\right)+\left(\frac{X}{l_r}-1\right)^2\right], \quad \text{for}$$

$$0 \le X \le l_r \quad (11)$$

$$\nu_{hu}(X) = -K_{hu} \exp\left(\frac{X}{l_r}-1\right)\left[\left(\frac{X}{l_r}-1\right)+\left(\frac{X}{l_r}-1\right)^2\right], \quad \text{for}$$

$$0 \le X \le l_r \quad (12)$$

where K_h and K_{hu} = slowly varying functions of X that will be scaled using the integral form of energy Eq. (8). These relations provide a local spatial distribution for diffusivity coefficients and it is important to note that this functional form ensures overall

Table 1. Numerical Evaluation of Integral Terms I_h, I_{hu}, and α_b for Typical Surf Zone Values of the Breaker Index γ

γ	0.5	0.6	0.7	0.8
I_h	0.044	0.038	0.030	0.020
I_{hu}	0.045	0.030	0.019	0.011
α_b	0.70	1.83	4.62	12.1

mass and momentum conservation over a breaking event because $\nu_h = \nu_{hu} = 0$ at outer bounds of the region where diffusive terms are active. Hence, extra terms only produce a local redistribution of mass and momentum under the breaker without any addition or extraction of these quantities.

The roller length can be estimated from Cointe and Tulin's theory of steady breakers (Cointe and Tulin 1994) but with the associated empirical parameter, β, adjusted using shallow water experiments by Cienfuegos (2005). It is useful to recast this expression in the following form:

$$\frac{e_r}{d} = \frac{l_r \tan \Phi}{d} = \frac{\beta^2}{2(1-\beta^2)}(1-\gamma) \simeq 0.865(1-\gamma) \quad (13)$$

where the adjusted value $\beta = 0.796$ has been used. Finally, in order to be able to integrate the left hand side of Eq. (8), we use the long wave approximation which states that

$$(U+c)h = c(h-d) \quad (14)$$

and assume a simple linear form for the average wave's front position where breaking terms are applied, i.e., (see Fig. 5)

$$h = \left(1 + \gamma/2 - \frac{X}{d}\tan \Phi\right)d, \quad \text{for} \quad 0 \le X \le l_r \quad (15)$$

Hence, the final scaling provided by energy Eq. (8) introduces two parameters which define local characteristics of surf zone waves, namely the breaker index, γ, and the mean breaker slope, Φ.

The integral of the left-hand side of Eq. (8) can be evaluated using relations (9)–(15). It is thus possible to write the following scaling law for coefficients K_h and K_{hu}:

$$(I_h K_h + I_{hu} K_{hu})c^2 \tan \Phi = \frac{1}{4}gc\gamma^3 d^2 \quad (16)$$

with I_h and I_{hu} integrals that are weakly dependent on γ defined as

$$I_h = -\int_0^1\left[\left(1+\frac{\gamma}{2}-\frac{e_r}{d}\tau\right)+\frac{1}{2}\left(1-\left(1+\frac{\gamma}{2}-\frac{e_r}{d}\tau\right)^{-1}\right)^2\right]\psi(\tau)d\tau \quad (17)$$

$$I_{hu} = -\int_0^1\left(1-\left(1+\frac{\gamma}{2}-\frac{e_r}{d}\tau\right)^{-1}\right)\psi(\tau)d\tau \quad (18)$$

with

$$\psi(\tau) = \exp(\tau-1)(\tau+\tau^2-1) \quad \text{for} \quad 0 \le \tau \le 1$$

where we have introduced the nondimensional variable, $\tau = X/l_r$. The ratio e_r/d can be estimated through Eq. (13) and a numerical integration can be performed in order to evaluate I_h and I_{hu} for different values of the breaking index, γ. Results are presented in Table 1, where it is seen that in the surf zone, both terms are of the same order with values ranging between 0.01 and 0.05.

The Eq. (16) follows directly from energetic considerations and has the merit of explicitly showing the relation between the
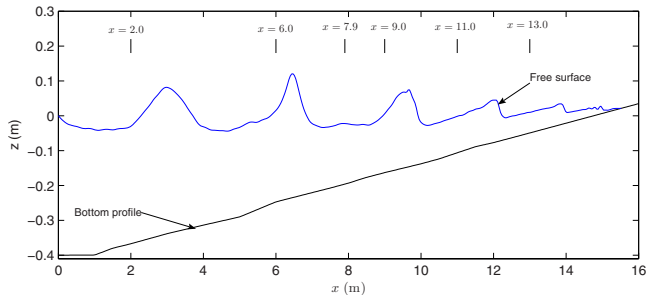
Fig. 6. Definition sketch for Ting and Kirby (1994) spilling breaking experiment, $H_0=0.127$ m, $L_0=3.74$ m, and $T=2.0$ s (computed results using the proposed breaking model). Vertical lines correspond to locations of wave gauges in meters.

eddy viscosity coefficients, K_h and K_{hu}, local wave parameters, γ, Φ, and the associated velocity and length scales, c and d. However, for practical applications, we will assume that $I_h=I_{hu}$, and that the ratio $\kappa=K_h/K_{hu}$ ($0 \leq \kappa \leq 1.0$) is constant. Using this in Eq. (16) provides the following expression for eddy viscosity coefficients:

$$K_{hu} = \delta \frac{cd}{\tan \Phi} \qquad (19)$$

$$K_h = \kappa \delta \frac{cd}{\tan \Phi} \qquad (20)$$

with

$$\delta = \frac{\alpha_b}{(1+\kappa)} \quad \text{and} \quad \alpha_b = \frac{\gamma^3}{4I_{hu}}$$

Numerical estimates for function α_b are presented in the last row of Table 1. It appears that α_b should take values of the order $O(1)-O(10)$ in the surf zone.

Parameter Calibration

In the breaking model, there are two main *physical* parameters to set, Φ and γ, but two additional coefficients, κ and α_b, need to be prescribed. Since, we do not have a clear knowledge of how these quantities may evolve inside the surf zone, the calibration process must be tackled with pragmatism in order to keep the model as simple as possible. In the following subsections we introduce the heuristic procedure that will allow us to determine optimal values for model parameters. Similarly, some aspects related to its practical implementation will be highlighted.

We recall that our main goal is to improve the time-domain representation of free-surface elevations in the surf zone, in particular wave height, asymmetry, and skewness estimates. On that purpose, we will use Ting and Kirby (1994) spilling breaking experiment to obtain parameter values which minimize the average error for H, As, and Sk. In this experimental setup, cnoidal waves with incident height $H_0=0.127$ m and period $T=2.0$ s propagate toward a planar beach of slope 1:35. The still water level was fixed at $h_0=0.4$ m in the horizontal part of the flume and phase-averaged time series of free-surface elevation are available at 21 locations, before and after breaking. This data set thus provides valuable information to test Boussinesq wave propagation models and breaking parameterizations. A sketch of the spatial configuration of the bottom bathymetry and the location of several wave gauges is presented in Fig. 6.

The heuristical calibration process is carried out using a grid size $\Delta x=0.1\ h_0$ and a Courant number $C_r=\sqrt{gh_0}\Delta t/\Delta x=1.0$, where h_0 is the still water depth in the horizontal part of the flume where the experiment is conducted, L_0 is the wavelength of incident waves, Δx and Δt are, respectively, spatial and temporal grid resolutions. In addition, the correction dispersion coefficient in SERR-1D is fixed at $\alpha=1/15$ thus producing a Padé (2,2) approximation for the Stokes dispersion relation (Cienfuegos et al. 2007).

Adopted Breaking Criteria

Concerning the breaking criteria, the different approaches reviewed in the second section were implemented in the finite volume model and their breaking point predictions analyzed. Details on this comparative study are not reported here but general conclusions were similar to those given by Lynett (2006) since a criterion based on the mean wave's front slope appeared to be the least sensitive when considering spilling breaking. Hence, our numerical implementation of the breaking model utilizes this criteria to decide when extra terms should be activated. In the moving frame of reference associated to each individual wave, threshold values for breaking initiation and cessation read

$$\text{breaking starts if} \left| \frac{d\eta}{dX} \right| \geq \tan \Phi_b$$

$$\text{breaking stops if} \left| \frac{d\eta}{dX} \right| \leq \tan \Phi_f$$

where $\Phi_b=$ limiting breaker angle for breaking inception and Φ_f = saturated breaker angle for which the breaking process stops. The front face slope is estimated from computed spatial derivatives of water depth and bottom bathymetry, where the maximum local value of $|d\eta/dX|$ over the spatial extent of the front face is considered as reference for each breaker.

Since the breaking parameterization is applied on a wave-by-wave basis, a numerical algorithm is considered in order to follow each wave crest. Furthermore, breaking terms are applied on the front face over an extent l_r starting at the wave crest (see Fig. 5). Diffusivity coefficients are spatially reconstructed using local functional forms (11) and (12).

Parameter Calibration Using a Spilling Breaking Experiment

The calibration of model parameters and coefficients is a difficult task owing to the great number of degrees of freedom and possible combinations for physical ranges of parameter values. We need to prescribe values for Φ, α_b, and κ, and the horizontal extent over which extra terms are applied. The latter is obtained from the wave's front slope and the breaker index through relation $l_r/d=0.865(1-\gamma)\tan^{-1}\Phi$, once values of γ and Φ are chosen. Finally, wave celerity will be computed as $c=\sqrt{gd}$, based on the still water depth $d=-\xi$ when $\xi<0$ (see Fig. 5).

An important property of the new breaking formulation concerns the possibility of explicitly defining the length of the segment where diffusivity terms are applied. Numerical experiments have shown that the horizontal asymmetry of predicted surf zone waves is strongly dependent on l_r. In particular, it was noticed that a combination of too large values for this horizontal scale with high magnitudes of eddy viscosity coefficients may produce important inaccuracies in left-right asymmetry estimates. Con-

versely, l_r has a lower bound given by the grid size resolution Δx and the minimum possible value for this distance is taken to be $l_r = 2\Delta x$ in the model. Therefore, a compromise between a good representation of wave asymmetry and practical aspects of numerical computations must be determined.

Concerning the relative weight of mass and momentum diffusivity terms, κ, numerical experiments show that the value for this coefficient needs to be chosen carefully since it appears that setup level is lowered if κ-values are greater than 0.3. On the other hand, empirical evidence indicates that the breaker index should be bounded by $0.4 \leq \gamma \leq 0.8$ over most of the surf zone according to Andersen and Fredsoe (1983) but may reach higher values in the swash zone [e.g., Raubenheimer et al. (1996)]. In the particular case of Ting and Kirby (1994) spilling breaking experiment, $\gamma = H/d$ ranged from 0.8 near the breaking point, down to a rather constant value of 0.5 in the inner surf zone. Similarly, the mean front slope of the breaker, Φ, should evolve from a high limiting value near the breaking point to a lower one as the breaker reach a quasi-equilibrium state in the inner surf zone (Govender et al. 2002; Schäffer et al. 1993). Unfortunately, there is no clear knowledge of what kind of temporal evolution function those quantities should follow. Therefore, in order to keep the breaking model at a reasonable level of complexity parameters γ and Φ and coefficients κ and α_b will be taken as constants over the entire surf zone. The calibration process must provide their optimal values within physical ranges. In addition, the two threshold values for breakers angles, Φ_b and Φ_f, need to be prescribed.

A large number of numerical experiments were conducted in order to determine the optimal parameter set but we only report here the main conclusions that can be drawn from this heuristic process:

1. Using a ratio $\kappa = K_h/K_{hu}$ greater than 0.3 produces an under estimation of setup level in the inner surf zone.
2. A combination of large l_r/d values with a strong magnitude for diffusivity coefficients produces small spurious oscillations behind breakers that can lead to numerical instability.
3. The limiting front slope for breaking initiation must be fixed such that $\Phi_b \sim 28° - 32°$ for spilling breakers or even reach $35° - 36°$ for strong plunging events.
4. The threshold value for breaking termination has no influence for Ting and Kirby experiment as long as it is fixed at a value $\Phi_f < 10°$.
5. The application of a 8th order compact implicit filter as given by Gaitonde et al. (1999) with $\alpha_f = 0.4$ improves the numerical performance of the scheme without significantly removing energy from the system [see Cienfuegos et al. (2007), for further details]. In the following applications the filter is used once per time step.

Numerical experiments have shown that concentrating breaking terms on a smaller horizontal distance near the top of the breaker results in better agreement with measured surface elevation profiles and left-right wave asymmetry. A good compromise between the numerical performance of the scheme and predicted properties of surf zone waves in the case of Ting and Kirby (1994) spilling breaking is achieved taking $\gamma = 0.8$, $\Phi = 13°$, $\kappa = 0.1$, and $\alpha_b = 5.0$ in the model. Parameters are kept constant over the whole surf zone, hence no transitional time scale is required. Finally, optimal threshold values for breaking inception and cessation are found to be $\Phi_b = 30°$ and $\Phi_f = 8.0°$.

Replacing optimal values for parameters and coefficients in definitions (19) and (20) implies that

$$K_{hu} = 20cd \qquad (21)$$

$$K_h = 2cd \qquad (22)$$

$$\frac{l_r}{d} = 0.82 \qquad (23)$$

which are used hereafter. It is important to note that slightly different values for breaker inception and diffusivity coefficients have been used in a different context (dam-break applications) by Mignot and Cienfuegos (2008).

For Ting and Kirby (1994) experiment, free-surface elevation time series are available at 21 locations, it is thus possible to compute an error index for predicted wave profiles over the whole domain. Following Kennedy et al. (2000) we compute left-right asymmetry as

$$As = \frac{\langle \mathcal{H}(\eta - \bar{\eta})^3 \rangle}{\langle (\eta - \bar{\eta})^2 \rangle^{3/2}} \qquad (24)$$

where $\langle \cdot \rangle$ = time-average operator and $\mathcal{H}$ = Hilbert transform. Similarly, crest-trough asymmetry or wave skewness is defined as

$$Sk = \frac{\langle (\eta - \bar{\eta})^3 \rangle}{\langle (\eta - \bar{\eta})^2 \rangle^{3/2}} \qquad (25)$$

A spatial snapshot of computed free-surface elevation in the case of Ting and Kirby (1994) experiment is plotted in Fig. 6 where it is clearly seen that the typical inner surf zone saw-tooth shape is well recovered. Wave-averaged properties produced by the model are reported in Fig. 7 and the agreement between measured and computed crest and trough levels is almost perfect. Results concerning intraphase properties at different locations are depicted in Fig. 8. RMS error on wave height predictions over the whole domain is nearly 8%, 22% for horizontal asymmetries, and roughly 15% for the skewness coefficient. Hence, the average RMSE over these three important quantities appears to be of roughly 15%, almost half of the error produced when using Kennedy et al. (2000) model on the same experiment.

It is worth noting that most of the modeling errors take place in the vicinity of the breaking point. This is more evident for the wave asymmetry coefficient since there are noticeable differences between computed and measured values in the transition zone. Nevertheless, the error is reduced in the inner surf zone thus proving that the proposed breaking model allows for a correct representation of wave height and asymmetry in this region.

A very important feature of the proposed model and the chosen set of parameters is that there is no transitional time scale. The latter constitutes a practical improvement compared with former breaking models [e.g., Kennedy et al. (2000) and Schäffer et al. (1993)] since it is not necessary to mark and follow individual breaking events in time. Nevertheless, knowledge on local front face breaker angle and crest location are still required. In the following subsection the proposed breaking model and the chosen set of parameters will be validated using several experimental benchmark tests.

Model Validation

In order to evaluate the ability of the new breaking model to predict surf zone wave properties we perform numerical computations for several experimental test cases keeping the same optimal set of parameter values obtained in the previous subsection. We consider Cox's regular wave experiment (Cox 1995), five different tests on regular waves shoaling and breaking on a planar beach conducted by Hansen and Svendsen (1979), and a solitary
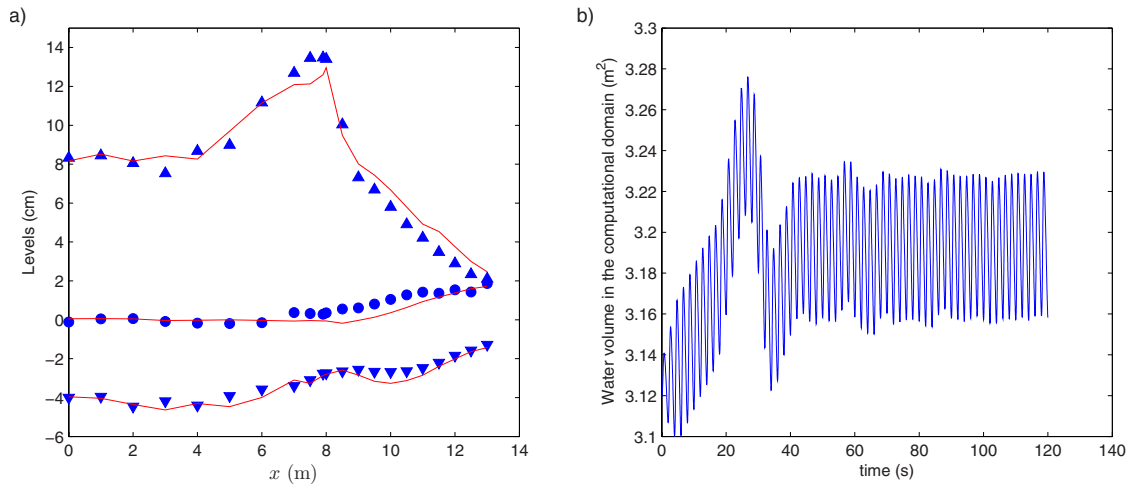
Fig. 7. Numerical predictions for Ting and Kirby (1994) spilling breaking experiment using the proposed breaking model. (a) (▲): measured crest level $\eta_c - \bar{\eta}$; (●): measured wave-averaged free surface $\bar{\eta}$; (▼): measured trough level $\eta_t - \bar{\eta}$; computed properties are plotted in solid lines; (b) temporal evolution of the water volume contained in the numerical domain.

wave breaking on a beach investigated by Synolakis (1987). All the following computations are carried out using a grid size $\Delta x = 0.1$ h_0 and a Courant number $C_r = \Delta t / \Delta x \sqrt{g h_0} = 1.0$, where h_0 is the still water depth in the horizontal part of the flumes where different experiments are conducted.

Application to Spilling Breaking Experiment

Cox (1995) conducted detailed measurements for cnoidal waves shoaling and breaking on a planar beach of slope 1:35. Wave

conditions are similar to Ting and Kirby (1994) spilling breaking case, except for a slightly longer period and a smaller incident wave amplitude. In addition, synchronized phase-averaged time series of free-surface elevations at six measuring sections are available. Hence, we can also investigate model performance in terms of phase speed prediction.

A comparison between predicted and measured setup, crest, and trough levels is presented in Fig. 9 where the theoretical cnoidal wave solution has been used to prescribe the incident free-surface time series at the left boundary, and the moving
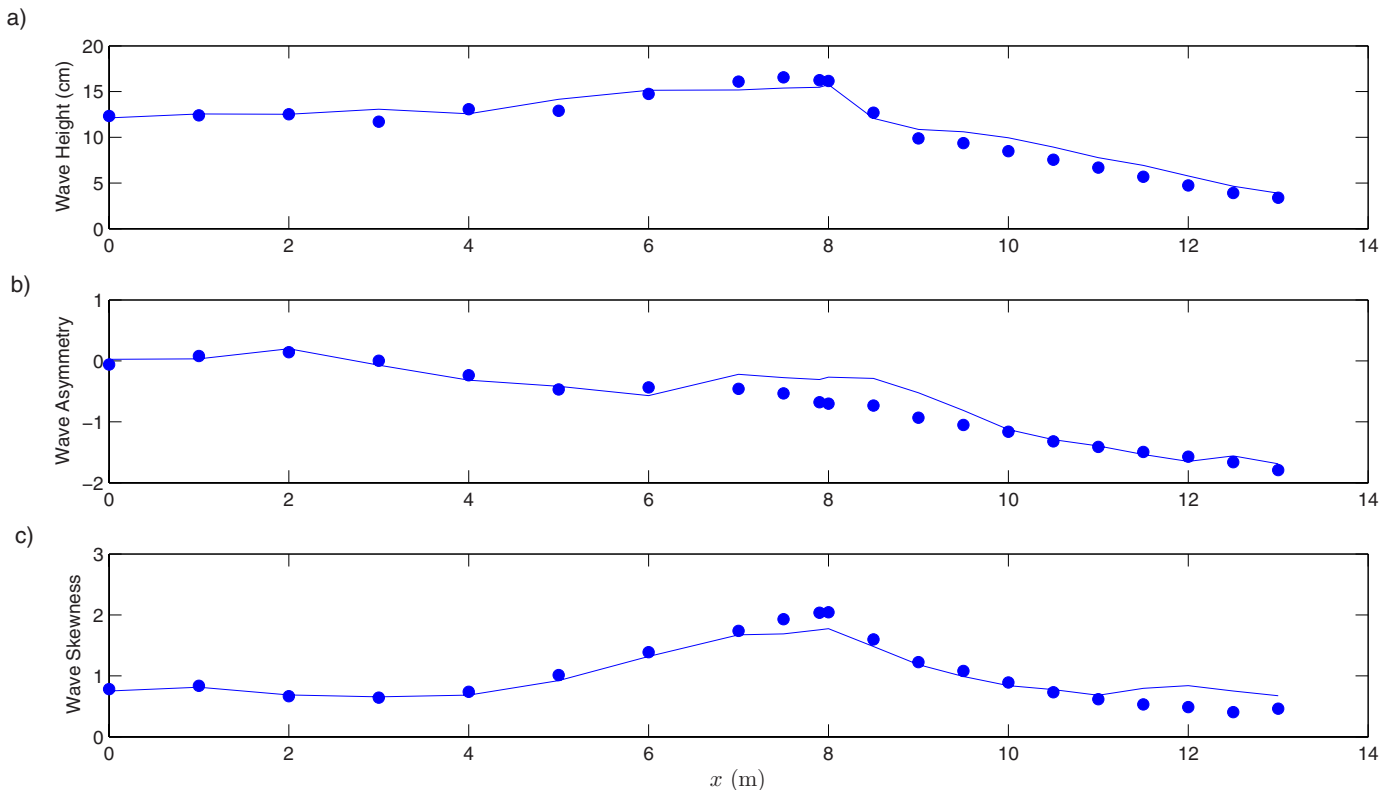
Fig. 8. Comparison between measured (●) and computed (–) wave properties for Ting and Kirby (1994) experiment using the proposed breaking model. (a) Wave height; (b) wave asymmetry; and (c) wave skewness.
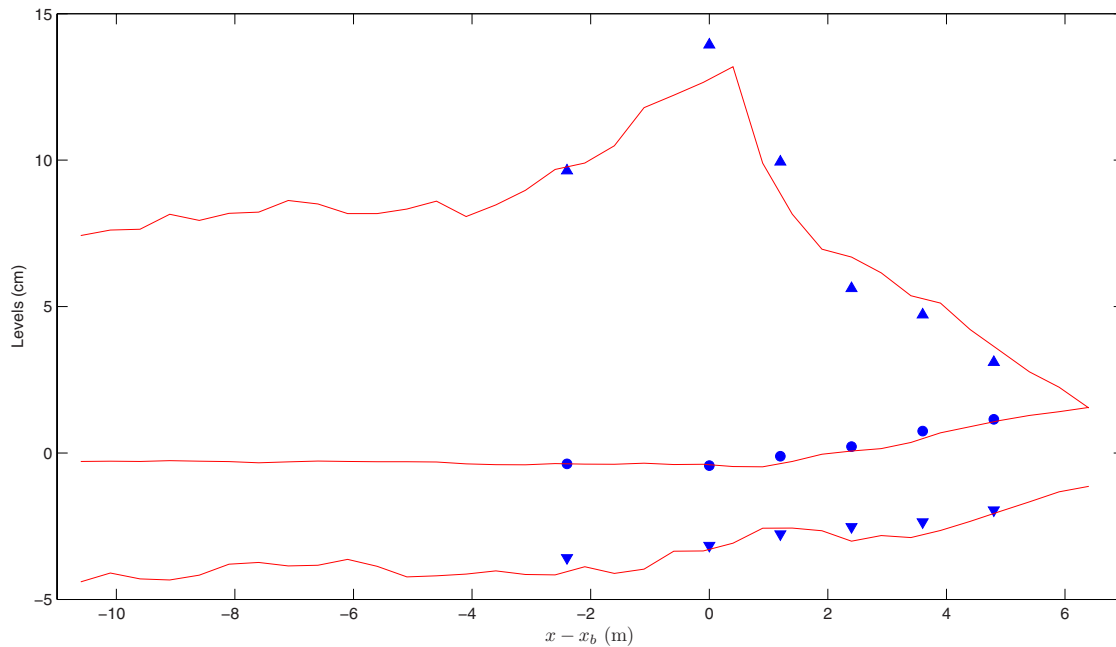
Fig. 9. Comparisons of model predictions and experimental data for Cox (1995) spilling breaking, H_0=0.115 m, L_0=4.19 m, T=2.2 s. (▲): measured crest level $\eta_c - \bar{\eta}$; (●): measured wave-averaged free surface $\bar{\eta}$; (▼): measured trough level $\eta_t - \bar{\eta}$. Computed properties are plotted in solid lines.

shoreline condition is implemented at the right boundary. Results compare very well with experimental data and an excellent non-linear performance in the shoaling region is noticed. Indeed, the breaking point location and the maximum wave height are accurately predicted. Similarly, surf zone wave height evolution is fairly well reproduced by the model.

Associated phase-averaged free-surface time series are reported in Fig. 10 for the six sections where measurements were conducted. The overall agreement between measured and computed time series is good thus confirming that the breaking model allows for a correct estimation of wave asymmetries and heights in the surf zone. However, there is a small phase shift in section $x - x_b$=4.8 m. Nevertheless, free-surface prediction is comparable to the one reported for the same experiment by Musumeci et al. (2005) using a much more complex Boussinesq model in which the irrotationality assumption was removed.

Model Performance for Hansen and Svendsen (1979) Benchmark Tests on Regular Waves

Hansen and Svendsen (1979) experiments on regular waves shoaling and breaking on a planar beach of slope 1:34.26 have become a benchmark test for Boussinesq-type equations and associated breaking parameterizations. For instance, Kennedy et al. (2000), Veeramony and Svendsen (2000), Briganti et al. (2004), and Musumeci et al. (2005) (among others) have used these data sets to validate time-domain breaking models. In addition, since a wide range of wavelengths were investigated by Hansen and Svendsen (1979), the available experimental information provides a good opportunity to test nonlinear shoaling characteristics of SERR-1D model.

We have chosen five test cases following Kennedy et al. (2000) validation procedure, for wave conditions producing breaker types ranging from gentle spilling to strong plunging events. Selected experimental series and their main characteristics are summarized in Table 2. Regular wave test cases range from

fairly short incident waves to rather long ones. The associated dispersion parameter for the shorter wavelength test is kh_0=1.58, thus almost one half of the theoretical limit of the extended system of Serre equations implemented in SERR-1D. Numerical examples reported in the following are carried out using theoretical second order Stokes waves as left boundary condition, while the moving shoreline is prescribed at the right boundary.

Numerical results for spilling breakers are presented from Figs. 11–14. It is seen that the breaking point location is reasonably predicted in all cases using the same numerical values for model parameters as inferred from Ting and Kirby (1994) measurements. Similarly, the shoaling region is fairly well described by the numerical model except in the vicinity of the breaking point where the limiting wave amplitude is slightly underpredicted. This trend was already noticed when calibrating the breaking model using Ting and Kirby (1994) experiment.

On the other hand, surf zone wave evolution is predicted in good agreement with experimental data. This is clearly observed in test cases No. 041041, No. 053074, and No. 061071 which have longer surf zone extensions. In particular, model performance in the inner surf zone is excellent since computed wave amplitudes follow the measured values with great accuracy. There are only minor differences in the transition zone, which are mostly due to the initial underestimation of the maximum wave height and slight errors in breakpoint location. Setup levels are also predicted in a satisfactory way for all spilling cases and the spatial lag between the breaking point position and the beginning of setup is also well reproduced.

In summary, model performance for the spilling breaking cases investigated so far appears to be very good for wave heights, setup levels, and breaking point locations. Moreover, the transition zone is also fairly well reproduced using a fixed set of parameter values. It seems then justified to infer that physical
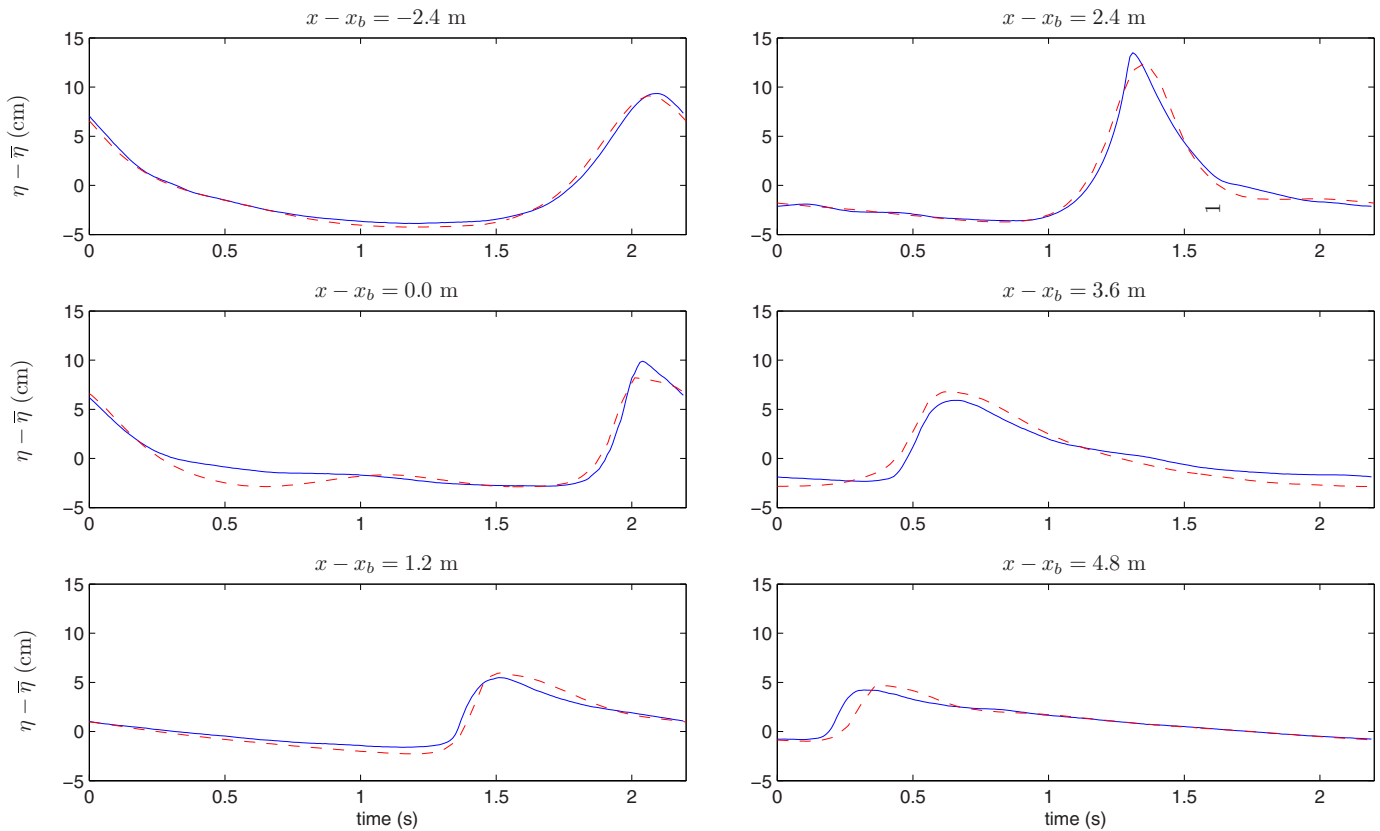
Fig. 10. Computed and measured phase-averaged time series of free-surface elevation at several wave gauges for Cox (1995) experiment. x_b is the coordinate for breaking initiation. (–): measured and (– –) computed.

arguments developed to derive scaling relations for the new breaking parameterization are quite robust thus providing accurate information for spilling breaking situations.

Comparisons between numerical computations and experimental measurements for the plunging case No. 031041 are reported in Fig. 15. The breaking point location is predicted slightly offshore than the measured one, but wave height evolution in the inner surf zone is correctly reproduced. Errors in the prediction of the breaking point location may be explained by the high nonlinear steepening of incident waves in the shoaling region. Indeed, the front slope threshold value, $\Phi_b = 30°$, was calibrated for spillinglike breakers and it follows from the previous discussion that for plunging events a higher limiting value for this property should be prescribed.

Several conclusions can be drawn from numerical computations presented in the present subsection. The first one concerns the ability of the breaking model to reproduce inner surf zone wave gradients even for plunging breakers and the fact that model behavior is rather insensitive to the chosen spatial grid resolution. Indeed a constant $\Delta x = 0.1\ h_0$ was used in computations where different wavelengths were investigated. This means that the

breaking parameterization succeeds in predicting an accurate energy dissipation despite the fact that the number of nodal points per wavelengths was not constant. This property suggests that the breaking model could be applicable even for random wave propagation problems [see Cienfuegos et al. (2006b)].

A second crucial feature concerns nonlinear shoaling characteristics of the extended set of Boussinesq-type equations implemented in SERR-1D. Numerical results prove that Serre equations possess an excellent nonlinear behavior since only a small underprediction of the maximum wave height ($<10\%$) could be noticed near the breaking point. We recall that additional shoaling experiments with solitary waves were reported by Cienfuegos et al. (2007) with similar conclusions.

Application to Solitary Wave Breaking on a Beach

The last experimental test case that we consider in order to validate the numerical model corresponds to a solitary wave propagating and breaking on a 1:20 constant slope beach as studied by Synolakis (1987). This author reported time series of incident and reflected solitary waves with a wave gauge located near the toe of

Table 2. Experimental Conditions for Selected Series of Hansen and Svendsen (1979) Regular Wave Test Cases

Test case	Wave period (s)	Wave height (cm)	$\epsilon = a_0 / h_0$	kh_0	Breaker type
A10112	1.02	6.7	0.093	1.580	Spilling
061071	1.68	6.7	0.093	0.791	Spilling
053074	2.02	6.6	0.092	0.641	Spilling
041041	2.53	3.9	0.054	0.501	Plunging-spilling
031041	3.37	4.3	0.060	0.369	Plunging
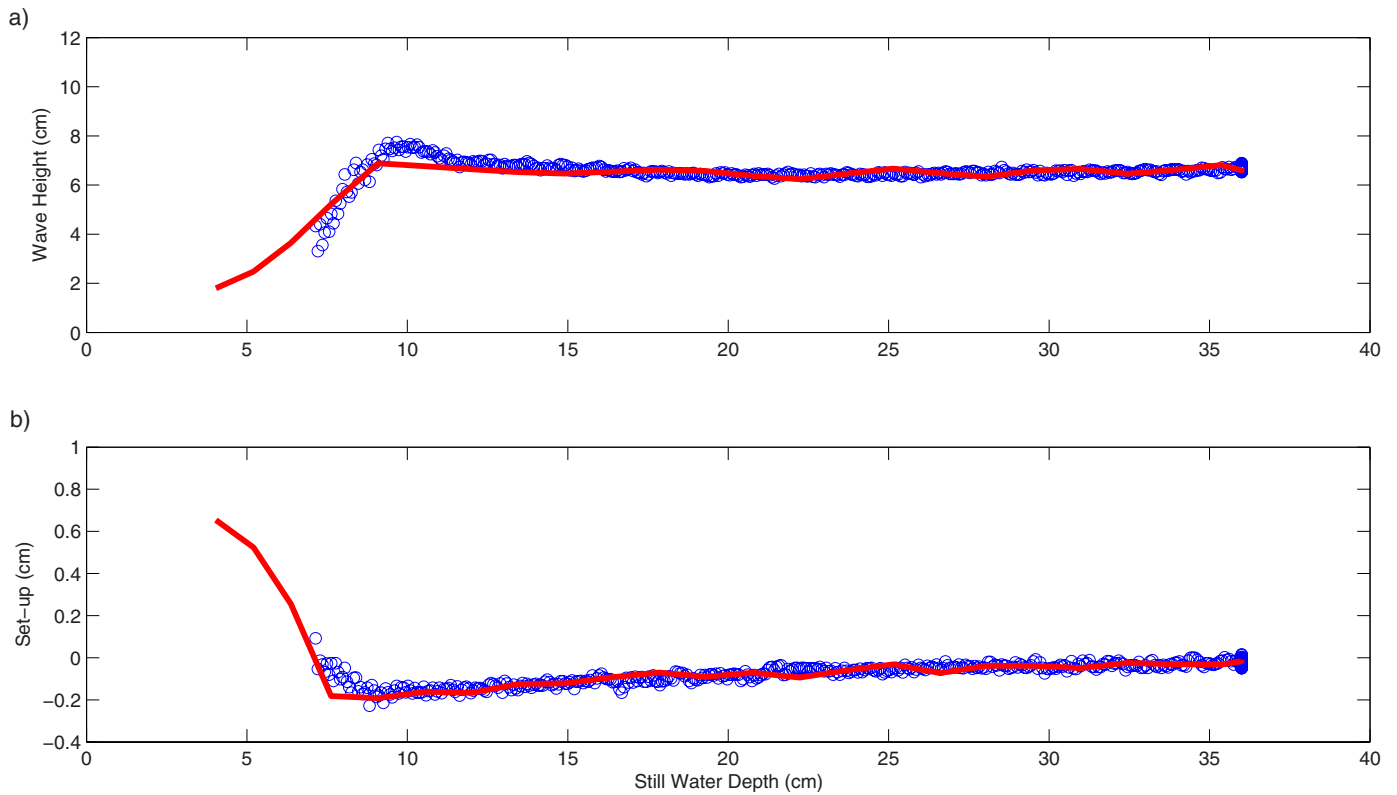
Fig. 11. Comparisons of model predictions and experimental data for Hansen and Svendsen (1979) spilling breaking test No. A10112. (○): measured data. Computed wave height and setup are plotted in solid lines.
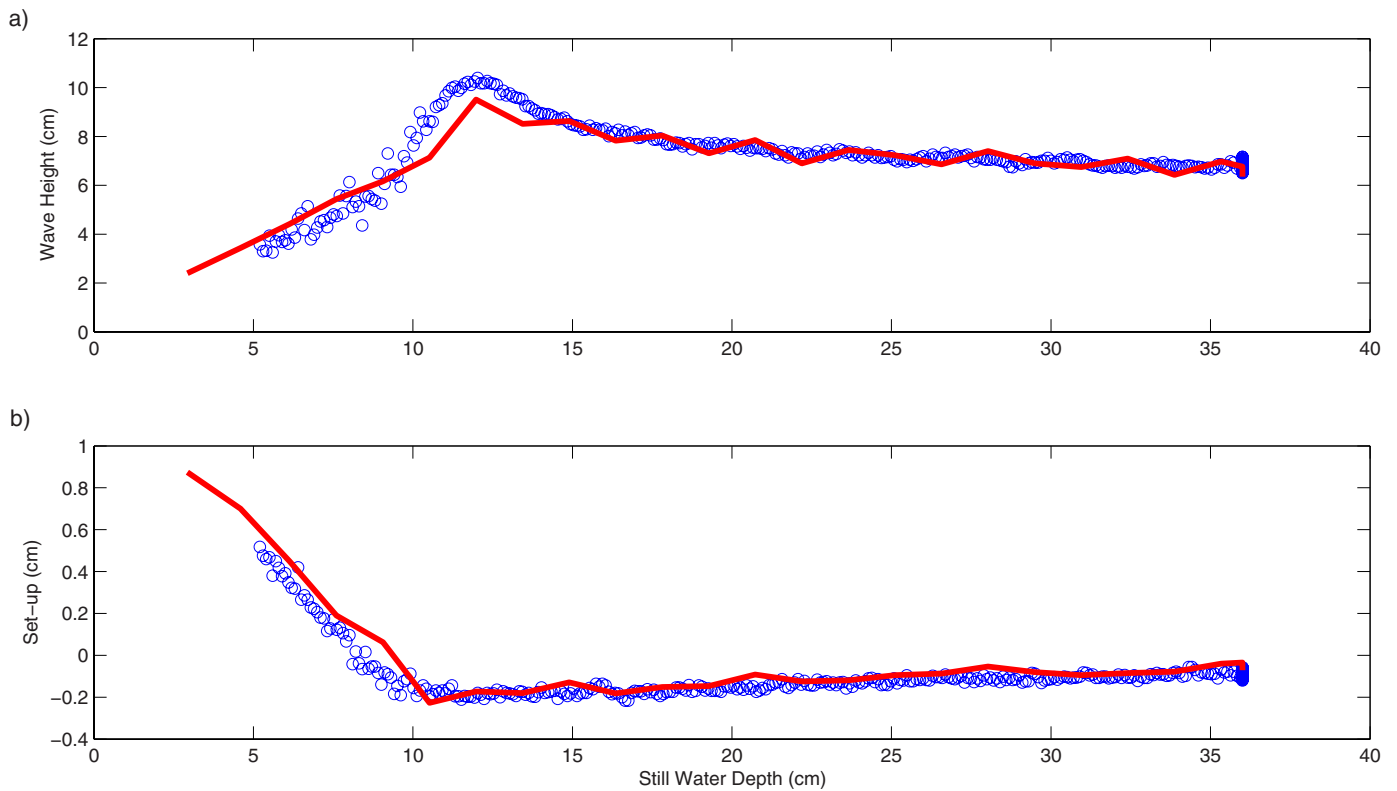
Fig. 12. Comparisons of model predictions and experimental data for Hansen and Svendsen (1979) spilling breaking test No. 061071. (○): measured data. Computed wave height and setup are plotted in solid lines.
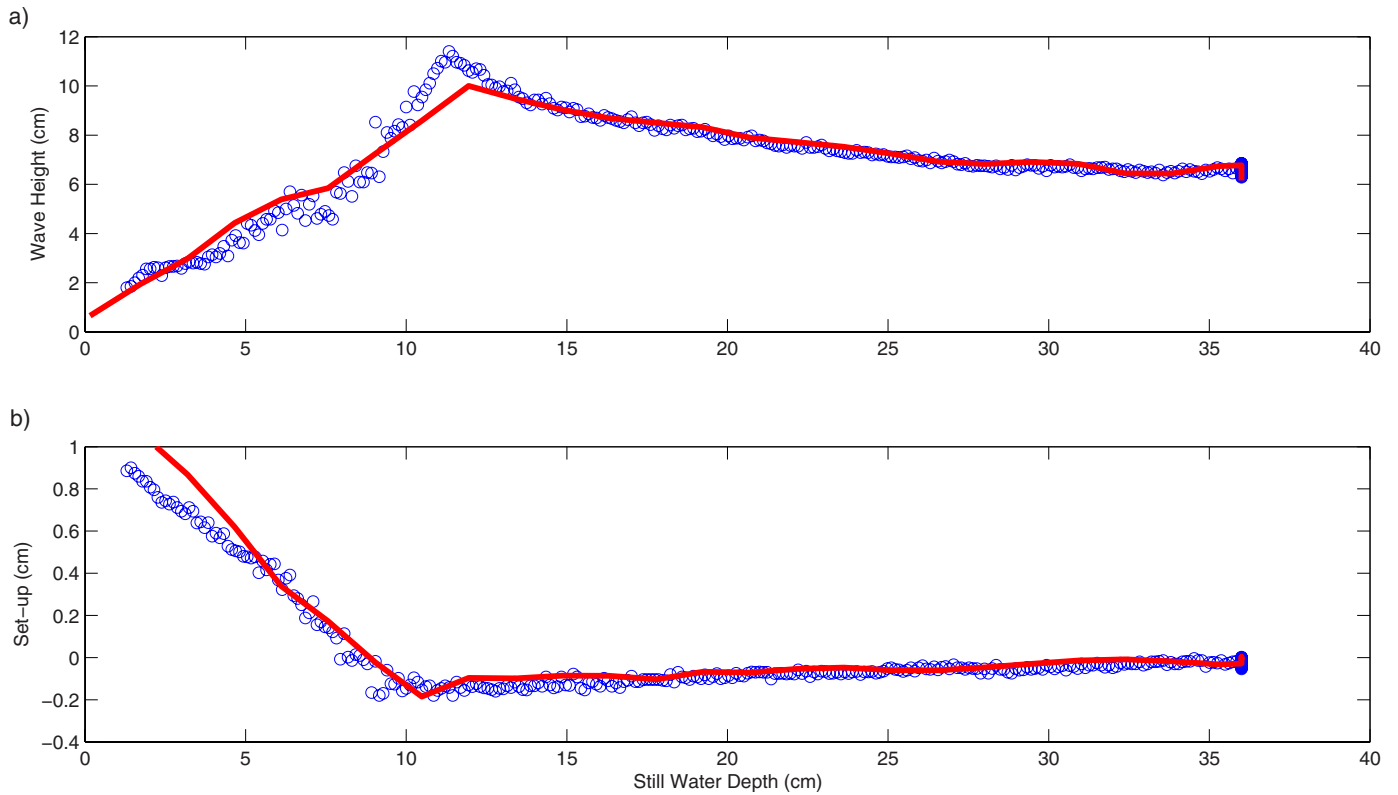
Fig. 13. Comparisons of model predictions and experimental data for Hansen and Svendsen (1979) spilling breaking test No. 053074. (○): measured data. Computed wave height and setup are plotted in solid lines.
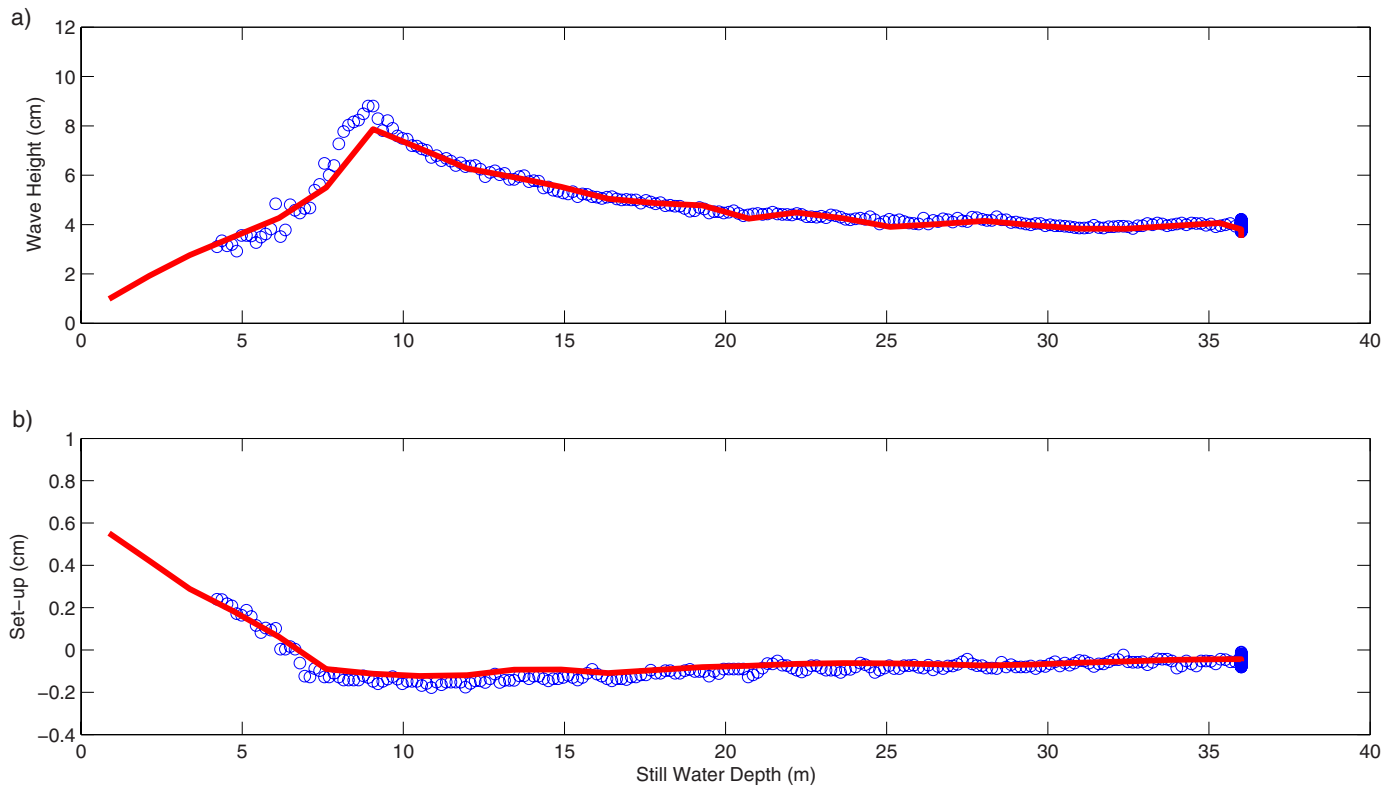
Fig. 14. Comparisons of model predictions and experimental data for Hansen and Svendsen (1979) plunging breaking test No. 041041. (○): measured data. Computed wave height and setup are plotted in solid lines.
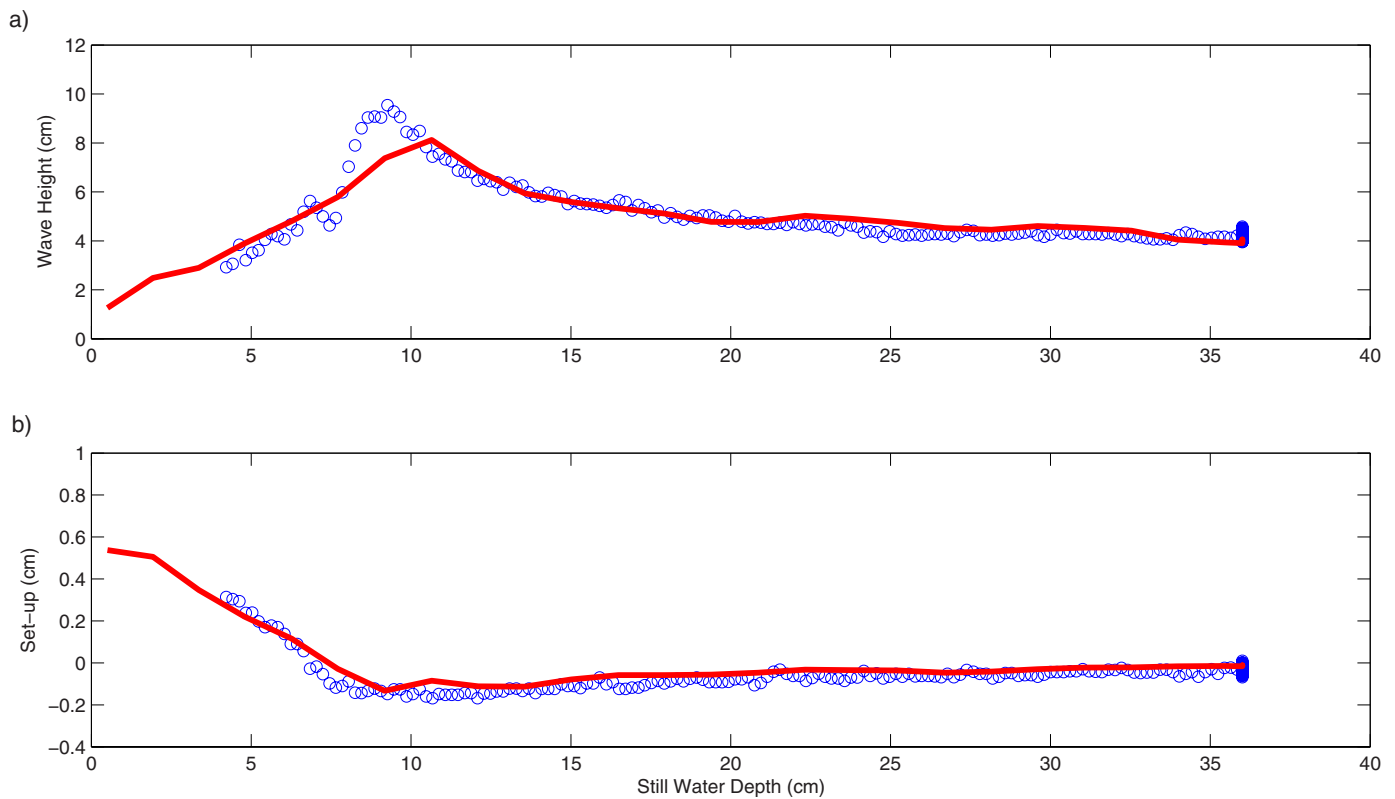
Fig. 15. Comparisons of model predictions and experimental data for Hansen and Svendsen (1979) plunging breaking test No. 031041. (○): measured data. Computed wave height and setup are plotted in solid lines.

the slope. This data was used to provide a common time origin for additional video measurements conducted for runup and rundown stages of nonbreaking and breaking solitary waves. Comparisons between predicted and measured spatial snapshots of propagating solitary waves were already reported for nonbreaking cases by Cienfuegos et al. (2007). Here we focus on a case with higher relative amplitude wave which broke strongly on runup. This particular experiment was also used by Zelt (1991) to test his breaking parameterization and the implemented Lagragian moving shoreline boundary condition.

The experimental case consists in a solitary wave with nondimensional incident amplitude $a_0/h_0=0.28$ propagating over a beach of 1:20 slope. The still water depth is fixed in the horizontal part of the wave flume at $h_0=0.25$ m for numerical computations reported in the following. The wave gauge located 4.775 m (=19.1 h_0) from the still shoreline is used to synchronize video measurements and numerical predictions. A comparison between available data at this location and computed results is presented in Fig. 16.

The breaking model is driven with the same parameter values determined using Ting and Kirby (1994) experiment. It is worth noting that video measurements produced by Synolakis (1987) allow for a detailed spatial comparison between experimental data and computed results. On the contrary, previous test cases studied in this section mostly concerned time-domain or wave-averaged properties so we have here an opportunity to test additional properties of the model. In particular, the ability of the implemented moving shoreline boundary condition to deal with strong breaking events will be investigated.

A free-surface time series comparison for numerical and experimental data are depicted in Fig. 16. It is seen that overall incident and reflected wave features are adequately reproduced by

the numerical model. Spatial snapshots of computed and measured free-surface profiles in runup and rundown stages are reported in Fig. 17. As pointed out by Zelt (1991), incipient breaking takes place slightly before the nondimensional time $t^*=t\sqrt{g/h_0}=20$ is reached. Prior to that time, the numerical model accurately predicts the solitary wave height and the nonlinear steepening of the incident soliton. Furthermore, inception of
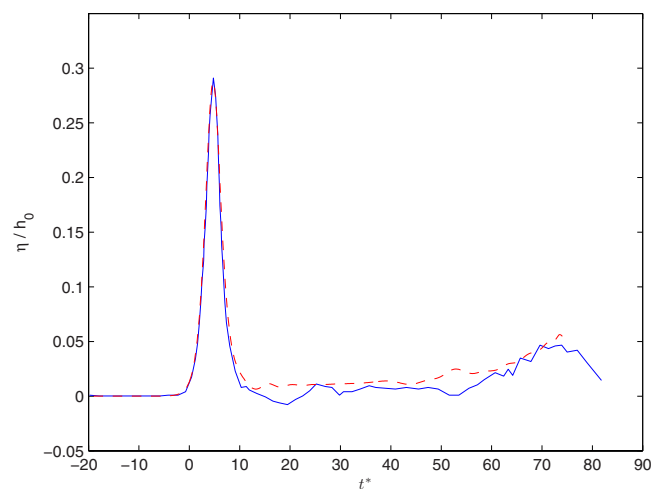
Fig. 16. Computed and measured incident and reflected solitary wave for the breaking case with $a_0/h_0=0.28$ investigated by Synolakis (1987). Wave gauge located 4.775 m from the still shoreline and $t^*=t\sqrt{g/h_0}$ is the nondimensional time. (–) measured time series, and (– –) predicted one using the numerical model.
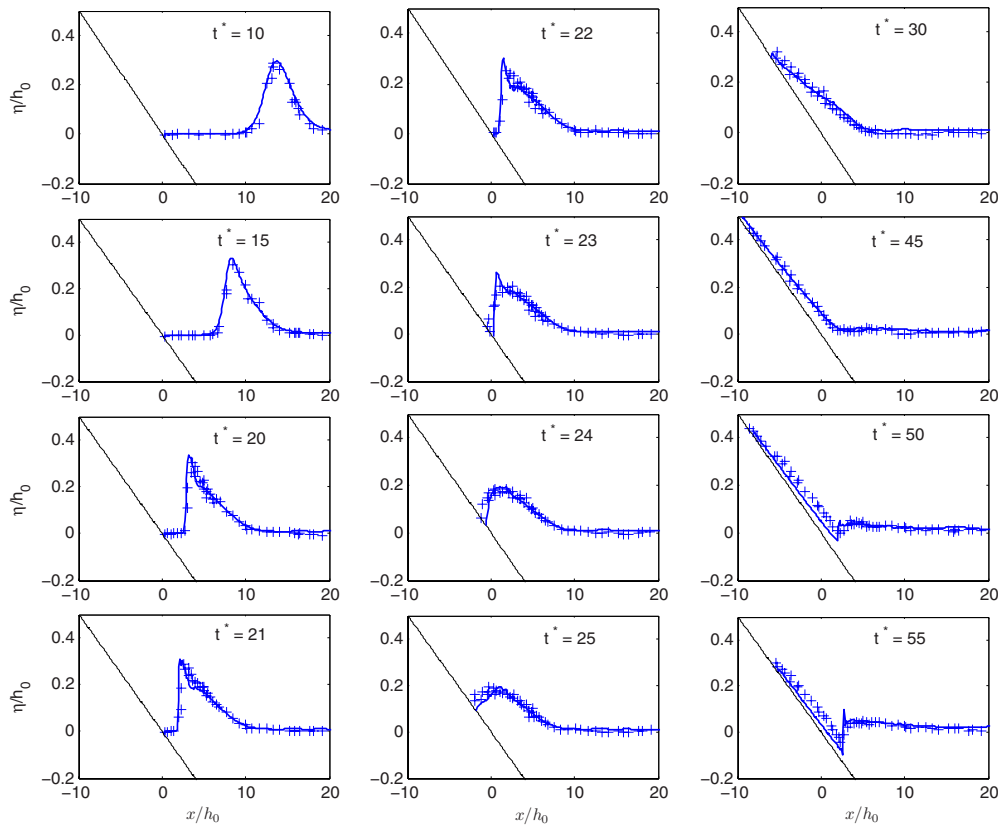
Fig. 17. Comparisons of model predictions and experimental spatial snapshots for the breaking solitary wave with $a_0/h_0 = 0.28$ investigated by Synolakis (1987). (+): experimental data, while numerical results are plotted in solid lines. $t\sqrt{g/h_0}$ is the nondimensional time.

breaking is also reasonably predicted by the model even when using parameter values obtained from a spilling breaking case. Again, embedded nonlinear characteristics of SERR-1D model provides very good agreement with experimental measurements near the incipient breaking location. It is worth noting that results reported by Zelt (1991) are slightly less accurate in terms of spatial wave shapes in the shoaling zone. More important, the overall agreement is quite good once breaking occurs between $t^* = 21$ and $t^* = 23$. Soon after, the solitary wave reaches the shoreline and the moving boundary condition starts acting. The runup stage is fairly well reproduced by the numerical model despite the fact that no friction parameterization is included in the governing equations. The latter is in contradiction with some of the conclusions given by Zelt (1991) who attributed some noticeable inaccuracies produced by his Lagrangian finite element model to friction effects. On the contrary, it is only in the rundown phase that slight discrepancies between experimental data and computed results can be observed in our case. Close inspection of free-surface evolution between panels $t^* = 45$ and $t^* = 55$ indicates that the numerical model produces a thinner water tongue than the measured one. This can be reasonably attributed to the lack of a friction term since friction effects are inversely proportional to water depths. Finally, it is observed in the last panel of Fig. 17 that a back swash breaking condition is reached and the numerical model is able to accurately reproduce this demanding situation where free-surface slope is almost vertical. However, it is important to recall that the breaking parameterization has not been conceived to handle this kind of breaking, thus an incipient spurious numerical behavior can be noticed in this last panel.

From this additional example, not only the ability of SERR-1D equations to deal with strong nonlinearities is satisfactorily con-

firmed, but also the physical and practical adequacy of the moving shoreline boundary condition described by Cienfuegos et al. (2007) is further validated for breaking cases.

Conclusions

The present paper has been devoted to the development and validation of a new time-domain breaking wave parameterization that may be used in the framework of Boussinesq-type equations. Our main concern was to improve the numerical representation of intraphase properties, such as asymmetry and skewness, specially in view of sediment transport prediction for beach morphodynamics. The model incorporates extra terms in both, the continuity and momentum equations which are applied on the front face of the breaker. These terms aim at introducing roller-induced effects, at a macroscopical scale, that are not otherwise taken into account by potential flow theory (turbulent mixing, flow separation in the roller region, etc.).

Invoking nonlinear shallow water shock theory, energetic considerations and experimental findings on quasi-steady hydraulic jumps investigated by Svendsen et al. (2000), we were able to find scaling relations for model parameters. This alternative approach, which is written as a function of the breaker index, γ, and the mean front slope, Φ, can be viewed as an extension of the eddy viscosity analogy used by Zelt (1991) and Kennedy et al. (2000). In particular, the extent over which breaking terms act, follows from a simple relation obtained by Cointe and Tulin (1994) and calibrated under experimental conditions more representative of inner surf zone waves by Cienfuegos (2005). It is

worth emphasizing that this relation introduces in the model an additional degree of freedom since the horizontal distance where diffusivity functions are applied is explicitly controlled. Indeed, numerical results obtained using constant values for model parameters over the entire surf zone, successfully demonstrated that wave heights and horizontal asymmetries could be accurately described. Moreover, the spatial lag between the breaking point and the location where setup starts was also reproduced by the numerical model.

On the other hand, it is important to stress that the calibration process performed on Ting and Kirby (1994) spilling breaking experiment, yields a breaking model which can deal with several different spilling breaking conditions using the same parameter values and without requiring a transitional time scale. Therefore, scaling arguments developed in the present work provide useful relations which seem to be more general than other forms used in former breaking wave parameterizations. Nevertheless, and in accordance to underlying hypothesis, breaking point location, and the spatial length of the transition zone occurring in plunging-type breakers could not be correctly captured using the same parameter set. This is mostly due to the higher steepening that longer period waves can reach, thus requiring a higher threshold value for the critical front slope. Similarly, in plunging events, intense energy dissipation takes place over a shorter distance producing a more rapid transitional behavior. In spite of that, inner surf zone wave height gradients were reasonably predicted by the model even for plunging breakers. We recall that the present model has been also applied to riverine configurations including dam-break flows with reasonable agreement between measurements and computations [see Mignot and Cienfuegos (2008)].

The physical adequacy of the implemented moving shoreline boundary condition, adapted from Lynett et al. (2002), was further validated using an experimental solitary wave breaking on a beach. Computed evolution for wave propagation in runup and rundown stages appeared to be in very good agreement with experimental measurements conducted by Synolakis (1987). Indeed, only slight discrepancies could be noticed in the rundown phase which may be reasonably explained by the lack of a friction term in the governing equations. Similarly, the different test cases investigated clearly confirmed that the extended system of Serre equations possesses excellent nonlinear characteristics since wave height evolution in the shoaling region was accurately reproduced. Only a minor underprediction, which was never larger than 10%, could be noticed near the breaking point in some cases.

Acknowledgments

References

Andersen, O., and Fredsoe, J. (1983). "Transport of suspended sediment along the coast." *Progress Rep. No. 54*, Institute of Hydrodynamics and Hydraulic Engineering, ISVA, Technical Univ. of Denmark, 33–46.

Barthélemy, E. (2004). "Nonlinear shallow water theories for coastal waves." *Surv. Geophys.*, 25(3–4), 315–337.

Bayram, A., and Larson, M. (2000). "Wave transformation in the nearshore zone: Comparison between a Boussinesq model and field data." *Coastal Eng.*, 39, 149–171.

Bonneton, P. (2001). "A note on wave propagation in the inner surf zone." *C. R. Acad. Sci. Paris*, 329, Série IIb 27–33.

Bonneton, P. (2007). "Modelling of periodic wave transformation in the inner surf zone." *Ocean Eng.*, 34, 1459–1471.

Briganti, R., Musumeci, R. E., Bellotti, G., Brocchini, M., and Foti, E. (2004). "Boussinesq modeling of breaking waves: Description of turbulence." *J. Geophys. Res.*, 109, C07015.

Brocchini, M., Drago, M., and Iovenitti, L. (1992). "The modeling of short waves in shallow waters. Comparisons of numerical models based on Boussinesq and Serre equations." *Proc., 23rd Int. Conf. Coastal Eng.*, ASCE, Reston, Va., 76–88.

Cienfuegos, R. (2005). "Modélisation numérique des houles bidimensionnelles et du déferlement bathymétrique." Ph.D. thesis, Institut National Polytechnique de Grenoble, Grenoble, France.

Cienfuegos, R., Barthélemy, E., and Bonneton, P. (2006a). "A fourth order compact finite volume scheme for fully nonlinear and weakly dispersive Boussinesq-type equations. Part I: Model development and analysis." *Int. J. Numer. Methods Fluids*, 51(11), 1217–1253.

Cienfuegos, R., Barthélemy, E., and Bonneton, P. (2006b). "Nonlinear surf zone wave properties as estimated from Boussinesq modelling: Random waves and complex bathymetries." *Proc., 30th Int. Conf. Coastal. Eng.*, ASCE, Reston, Va.

Cienfuegos, R., Barthélemy, E., and Bonneton, P. (2007). "A fourth order compact finite volume scheme for fully nonlinear and weakly dispersive Boussinesq-type equations. Part II: Boundary conditions and validation." *Int. J. Numer. Methods Fluids*, 53(9), 1423–1455.

Cointe, R., and Tulin, M. (1994). "A theory of steady breakers." *J. Fluid Mech.*, 276, 1–20.

Cox, D. (1995). "Experimental and numerical modeling of surf zone hydrodynamics." Ph.D. thesis, Univ. of Delaware, Newark, Del.

Dally, W., and Brown, C. (1995). "A modeling investigation of the breaking wave roller with application to cross-shore currents." *J. Geophys. Res.*, 100(C12), 24873–24883.

Deigaard, R., and Fredsøe, J. (1989). "Shear stress distribution in dissipative water waves." *Coastal Eng.*, 13, 357–378.

Gaitonde, D., Shang, J., and Young, J. (1999). "Practical aspects of higher-order numerical schemes for wave propagation phenomena." *Int. J. Numer. Methods Eng.*, 45, 1849–1869.

Govender, K., Mocke, G. P., Alport, M. J. (2002). "Video-imaged surf zone wave and roller structures and flow fields." *J. Geophys. Res.*, 107(C7), 3072.

Hansen, J. B., and Svendsen, I. A. (1979). "Regular waves in shoaling water: Experimental data." *Technical Report, ISVA Series*, Paper 21.

Karambas, T., and Koutitas, C. (1992). "A breaking wave propagation model based on the Boussinesq equations." *Coastal Eng.*, 18, 1–19.

Kennedy, A., Chen, Q., Kirby, J., and Dalrymple, R. (2000). "Boussinesq modeling of wave transformation, breaking and runup. I: 1D." *J. Waterway, Port, Coastal, Ocean Eng.*, 126(1), 39–48.

Kirby, J., and Kaihatu, J. (1996). "Structure of frequency domain models for random wave breaking." *Proc., 25th Int. Conf. Coastal Eng.*, ASCE, Reston, Va, 1114–1155.

Kobayashi, N., De Silva, G., and Watson, K. (1989). "Wave transformation and swash oscillation on gentle and steep slopes." *J. Geophys. Res.*, 94, 951–966.

Lynett, P. (2006). "Nearshore wave modeling with high-order Boussinesq-type equations." *J. Waterway, Port, Coastal, Ocean Eng.*, 132, 348–357.

Lynett, P., Wu, T., and Liu, P. (2002). "Modeling wave runup with depth-integrated equations." *Coastal Eng.*, 46, 89–107.

Madsen, P., Sørensen, O., and Schäffer, H. (1997a). "Surf zone dynamics simulated by a Boussinesq-type model: Part I. Model description and

cross-shore motion of regular waves." *Coastal Eng.*, 32, 255–288.

Madsen, P., Sørensen, O., and Schäffer, H. (1997b). "Surf zone dynamics simulated by a Boussinesq-type model: Part II. Surf beat and swash oscillations for wave groups and irregular waves." *Coastal Eng.*, 32, 289–319.

Mignot, E., and Cienfuegos, R. (2009). "On the application of a Boussinesq model to river flows including shocks." *Coastal Eng.*, 56(1), 23–31.

Musumeci, R., Svendsen, I., and Veeramony, J. (2005). "The flow in the surf zone: A fully nonlinear Boussinesq-type approach." *Coastal Eng.*, 52, 565–598.

Okamoto, T., and Basco, D. (2006). "The relative trough Froude number for initiation of wave breaking: Theory, experiments and numerical model confirmation." *Coastal Eng.*, 53(8), 675–690.

Ozanne, F., Chadwick, A., Huntley, D., Simmonds, D., and Lawrence, J. (2000). "Velocity predictions for shoaling and breaking waves with a Boussinesq-type model." *Coastal Eng.*, 41, 361–397.

Raubenheimer, B., Guza, R., and Elgar, S. (1996). "Wave transformation across the inner surf zone." *J. Geophys. Res.*, 101(C11), 25589–25598.

Schäffer, H., Madsen, P., and Deigaard, R. (1993). "A Boussinesq model for waves breaking in shallow water." *Coastal Eng.*, 20, 185–202.

Seabra-Santos, F., Renouard, D., and Temperville, A. (1987). "Numerical and experimental study of the transformation of a solitary wave over a shelf or isolated obstacle." *J. Fluid Mech.*, 176, 117–134.

Svendsen, I. (1984). "Mass flux and undertow in a surf zone." *Coastal Eng.*, 8, 347–365.

Svendsen, I., Madsen, P., and Hansen, J. (1978). "Wave characteristics in the surf zone." *Proc., 16th Int. Conf. Coastal Eng.*, ASCE, Reston, Va, 520–539.

Svendsen, I., Veeramony, J., Bakunin, J., and Kirby, J. (2000). "The flow in weak turbulent hydraulic jumps." *J. Fluid Mech.*, 418, 25–57.

Synolakis, C. (1987). "The runup of solitary waves." *J. Fluid Mech.*, 185, 523–545.

Ting, F., and Kirby, J. (1994). "Observation of undertow and turbulence in a laboratory surf zone." *Coastal Eng.*, 24, 51–80.

Veeramony, J., and Svendsen, I. (2000). "The flow in surf-zone waves." *Coastal Eng.*, 39, 93–122.

Vincent, S., Caltagirone, J.-P., and Bonneton, P. (2001). "Numerical modelling of bore propagation and run-up on sloping beaches using a MacCormack TVD scheme." *J. Hydraul. Res.*, 39(1), 41–49.

Zelt, J. (1991). "The run-up of nonbreaking and breaking solitary waves." *Coastal Eng.*, 15, 205–246.